

The interaction of pyrite with solutions containing silver ions

A. N. BUCKLEY, H. J. WOUTERLOOD

CSIRO Division of Coal Technology, PO Box 136, North Ryde, NSW 2113, Australia

R. WOODS

CSIRO Division of Mineral Products, PO Box 124, Port Melbourne, Vic 3207, Australia

Received 22 November 1988

Linear potential sweep voltammetry and X-ray photoelectron spectroscopy have been used to determine the products of the interaction of pyrite with sulphuric acid solutions containing silver ions. Silver sulphide was found to be the principal product for all reaction times. Initially, some sulphur excess (metal deficiency) in the sulphide lattice was associated with the formation of silver sulphide. The presence of elemental silver in addition to silver sulphide after extended reaction times was evident from the characteristics of voltammograms. This elemental silver was not detected by electron spectroscopy because it was formed as crystallites occupying only a very small area of the surface of the silver sulphide-covered pyrite. Silver sulphide was the only surface silver species present on a pyrite surface during acid iron(III) leaching; elemental sulphur was also identified on such surfaces.

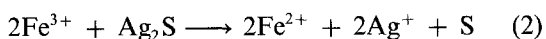
1. Introduction

There is current interest in the oxidative acid leaching of pyritic ores and concentrates prior to cyanidation in order to improve the recovery of precious metals disseminated in the pyrite matrix. While it is generally desirable for leaching to be carried out under conditions that produce elemental sulphur, the resultant layer formed on the pyrite surface limits the leaching rate and may lead to passivation [1]. Such inhibition has been observed for other sulphide minerals and, although it is commonly assumed that elemental sulphur is responsible for retarding electron transfer from the sulphide to the leachant, there is evidence that the presence of an intermediate layer of a metal-deficient sulphide is the rate-limiting factor [2-5].

The addition of low concentrations of silver ions has been shown to increase the rate of leaching of chalcopyrite [6] and sphalerite [7] in iron(III) solutions. The mechanism of silver catalysis has been attributed [6] to the formation of silver sulphide on the mineral surface:



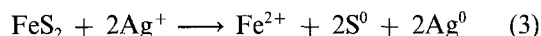
followed by oxidation of the silver sulphide by iron(III):



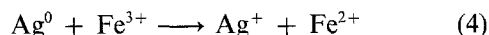
Acceleration of the overall process was considered to arise from the formation of a porous non-protective sulphur layer in Reaction 2, instead of a dense tenacious layer in the absence of the catalyst. An alternative explanation of the role of silver sulphide is that it provides cathodic sites on the mineral surface at which more rapid electron transfer can occur than on one

coated with an intermediate, polysulphide or metal-deficient sulphide product layer [3].

Recently, the possibility has been investigated [8] of producing an analogous increase in the oxidation rate of pyrite by the addition of silver ions to an acidic iron(III) sulphate leach solution. That investigation, which included the application of X-ray photoelectron spectroscopy (XPS), led to the conclusion that silver ions react with pyrite to form elemental silver and elemental sulphur as primary products:



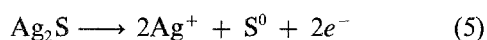
The formation of silver sulphide was also identified, but it was considered that this species appeared only as a minor product. Elemental silver subsequently would be oxidized by iron(III):



The Ag(3d) photoelectron and X-ray excited Ag(MNN) Auger electron spectra from small pyrite particles after treatment with silver ions in sulphuric acid solution appeared to indicate the presence of silver oxide, although silver sulphide could not be ruled out because of the unavailability of the Auger energies for this material. The silver oxide was believed to have been formed by aerial oxidation of elemental silver during the time between its formation and the analysis. This is an unexpected result since, while silver is oxidized by atomic oxygen [9], molecular oxygen may be adsorbed as a surface layer but does not oxidize it at ambient temperature [10]. Elemental sulphur or silver sulphide should be distinguishable from pyrite in the sulphur photoelectron spectrum. However, a high resolution sulphur spectrum was not reported for pyrite after treatment with silver ions [8].

The mechanism of pyrite oxidation represented by Reactions 3 and 4 was justified [8] in terms of an Eh/pH diagram which showed that elemental silver is the thermodynamically stable species at the rest potential of pyrite in solutions containing silver ions. However, the reported diagram also showed sulphate to be the stable sulphur species in this potential region, whereas Reaction 3 assumes that elemental sulphur is produced under the prevailing conditions. If sulphur is considered to have metastable existence in the system, then the Eh/pH diagram will display a metastable Ag_2S domain extending to potentials much greater than that for the dissolution of silver metal [11]. Thus, the co-existence of elemental silver and elemental sulphur is not supported by thermodynamic considerations.

The conclusion [8] that elemental silver is formed on the surface of pyrite when the mineral is immersed in sulphuric acid solutions containing Ag^+ was supported by electrochemical studies [12]. These investigations concentrated on the behaviour of pyrite electrodes in the potential region of the Ag^0/Ag^+ couple. As pointed out by the authors, the presence of silver sulphide could not be detected from the characteristics of its oxidation by:



because this process occurs in the same potential region as that for the oxidation of pyrite. However, consideration of the thermodynamics of the cathodic reduction of silver sulphide:



and of that of pyrite to iron metal or an iron sulphide of lower sulphur content, together with examination of voltammograms recorded for these systems [13, 14], indicates that it should be possible to detect the presence of silver sulphide on pyrite voltammetrically from its reduction behaviour. It is also possible to determine by this technique the presence on pyrite surfaces of elemental sulphur or excess sulphur in the form of a metal-deficient sulphide [14].

In the present communication, XPS and voltammetry have been applied to determine the conditions under which elemental sulphur, elemental silver and silver sulphide are formed by the interaction of pyrite with silver ions. Large, single particles of pyrite were used in the XPS investigations and this allowed the mineral to be maintained at a sufficiently low temperature while in the spectrometer to prevent volatilization of any elemental sulphur present on the surface. Photoelectron spectra for silver metal and precipitated silver sulphide were also determined under the same spectrometer conditions for comparative purposes.

2. Experimental details

Massive, high-purity crystals of pyrite from Navajun, Spain were used for the XPS studies and for the construction of pyrite electrodes. The bulk analysis of this material has been reported elsewhere [15].

Surfaces were abraded under nitrogen-saturated water immediately before immersion in the silver solution under investigation. Samples for XPS analysis were of approximate size $8 \times 8 \times 1$ mm. The exposed area of the pyrite electrode was 42 mm^2 . Some electrochemical studies using pyrite particles were carried out with mineral from Gumeracha, South Australia. Silver sulphide was prepared under nitrogen by precipitation from solutions of silver nitrate and sodium sulphide at about pH 9.

X-ray photoelectron spectra were obtained with a Vacuum Generators ESCA 3 spectrometer at an analyser pressure of 10^{-7} Pa. Unmonochromatized X-rays from a magnesium source operated at 10 kV, 10 mA were used. Spectra were determined with an analyser pass energy of 20 eV and slit width of 2 mm. Under these conditions, the $4f_{7/2}$ peak from gold has a width of 1.05 eV and a binding energy of 83.8 eV. Specimens were cooled to 150 K under nitrogen before evacuation, and maintained at this temperature at least until an initial S(2p) spectrum had been recorded. No peak shifting due to charging of the surface under X-ray irradiation was observed. Spectra are shown as raw data normalized by the difference between the maximum and minimum number of counts. S(2p) spectra were fitted with doublets with Gaussian-shaped (1/2, 3/2) components constrained to an intensity ratio of 1:2 and a separation of 1.19 eV. The binding energy of the $2p_{3/2}$ component is used to represent a S(2p) doublet energy.

The procedures used for the preparation of mineral electrodes, and the instrumentation used for voltammetry, are described elsewhere [16]. Voltammetry was also carried out on pyrite particles using a Metrohm carbon paste electrode. For this purpose, the particles were placed on a glass slide and imbedded into the electrode surface by pressing the electrode against the coated slide. Potentials were measured against a saturated calomel electrode (SCE); all potentials reported have been converted to the standard hydrogen electrode (SHE) scale on the basis that the SCE has a potential of 0.245 V [17] on this scale.

Scanning electron microscopy (SEM) examination was carried out using a JOEL 25S microscope equipped with a Link System energy dispersive spectrometer for quantitative elemental analysis.

3. Results and discussion

3.1. X-ray photoelectron spectra

S(2p) spectra recorded for elemental sulphur, a fresh pyrite surface, and precipitated silver sulphide are shown in Fig. 1A–C, respectively. It can be seen that there are significant differences in the S(2p) binding energies for these three species, *viz.* S^0 , 163.5 eV; FeS_2 , 162.4 eV; and Ag_2S , 161.3 eV.

The S(2p) spectrum, determined at 150 K, for pyrite after immersion for 2 h in 0.25 mol dm^{-3} sulphuric acid containing $10^{-2} \text{ mol dm}^{-3}$ silver ions at 350 K (Fig. 1D), consists predominantly of a doublet

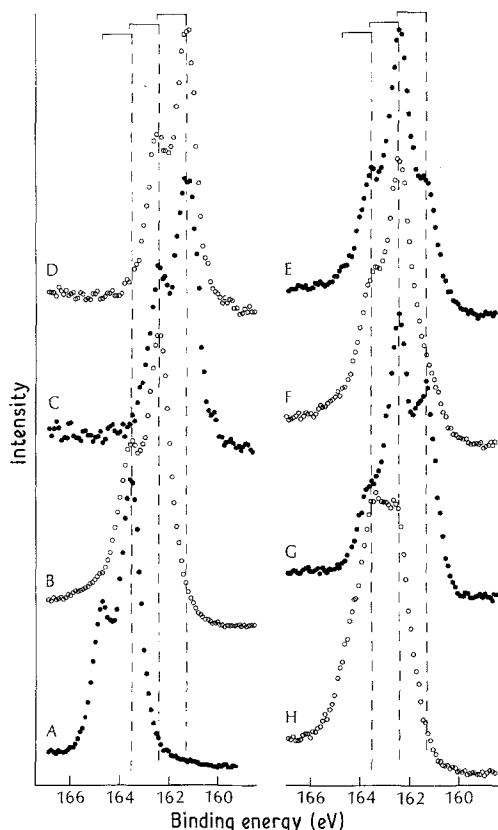


Fig. 1. S(2p) spectra determined at 150 K from (A) elemental sulfur; (B) pyrite; (C) silver sulfide; (D)–(H) pyrite surfaces treated for: (D) 2 h at 350 K in $0.25 \text{ mol dm}^{-3} \text{ H}_2\text{SO}_4$, $10^{-2} \text{ mol dm}^{-3} \text{ Ag}^+$; (E) 1 h at 298 K in same solution composition as in D; (F) 5 min at 298 K in $0.25 \text{ mol dm}^{-3} \text{ H}_2\text{SO}_4$, $10^{-3} \text{ mol dm}^{-3} \text{ Ag}^+$; (G) 15 h at 298 K in same solution composition as D and E; (H) 10 min at 298 K in unacidified $10^{-3} \text{ mol dm}^{-3} \text{ Ag}^+$ followed by immersion for 30 min at 350 K in $0.25 \text{ mol dm}^{-3} \text{ H}_2\text{SO}_4$, $1 \text{ mol dm}^{-3} \text{ Fe}_2(\text{SO}_4)_3$.

at 161.3 eV. A fitted component at 162.4 eV (Fig. 2), accounting for less than 10% of the total S(2p) intensity, would have arisen from a small amount of pyritic sulphur remaining within the depth analysed (about 5 nm for this energy) of at least part of the specimen surface. Elemental sulphur was not detected. An intense $\text{Ag}(3d)_{5/2}$ peak was observed (Fig. 3) and this had the same binding energy as precipitated silver sulphide (368.0 eV). $\text{Fe}(2p)$ photoelectron peaks were absent; thus, the sulphur species in the outermost layers (about 3 nm) was a silver sulphide and not an iron–silver sulphide. The escape depth for $\text{Fe}(3p)$ photoelectrons is greater than that for $\text{Fe}(2p)$. An

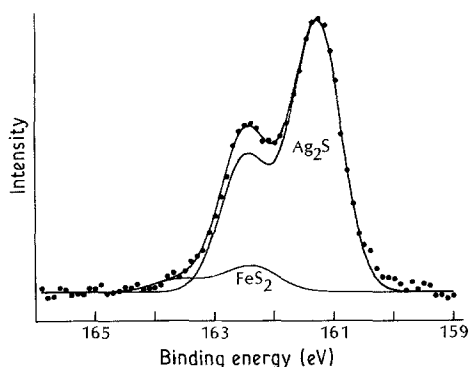


Fig. 2. Spectrum (D) of Fig. 1 fitted with doublets from pyrite and silver sulfide.

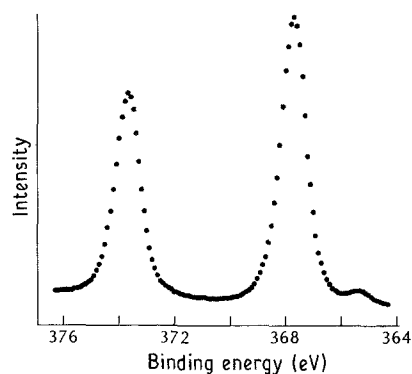


Fig. 3. $\text{Ag}(3d)$ photoelectron spectrum from pyrite treated with Ag^+ .

$\text{Fe}(3p)$ peak could just be detected adjacent to the broad $\text{Ag}(4p)$ peak and had an intensity corresponding to that of the residual pyritic sulphur. The alteration of virtually the entire depth analysed was not surprising, as the surface of the mineral had darkened noticeably after the treatment.

The $\text{Ag}(MNN)$ spectrum for the treated pyrite (Fig. 4A) is consistent with the surface being predominantly silver sulphide. The $\text{Ag}(M_4N_{4,5}N_{4,5})$ peak is at an energy of 357.0 eV which is the same as that found for silver sulphide (Fig. 4B). It is significantly different from the equivalent peak for silver metal, which has an energy of 358.1 eV (Fig. 4C). The presence of a small amount of elemental silver on the treated pyrite surface could not be ruled out; Auger kinetic energies for elemental silver are 1.1 eV greater than those for silver sulphide, but an M_4NN peak is relatively broad and contains a shoulder, due to 3P_2 and $^3F_{2,3}$ final state electron configurations, shifted about 1.4 eV to higher kinetic energy from the most intense 1D_2 , 1G_4 component. Similarly, the presence of a small amount of

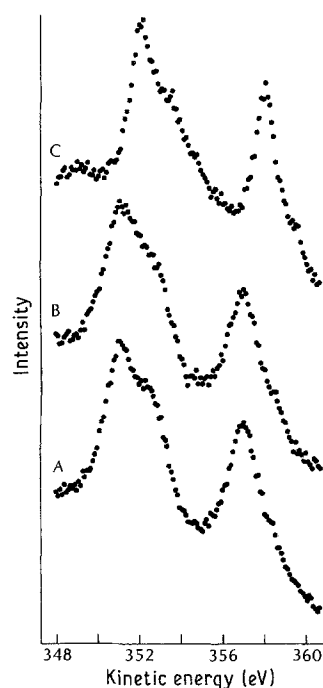


Fig. 4. $\text{Ag}(MNN)$ Auger spectra from: (A) pyrite treated with Ag^+ ; (B) precipitated Ag_2S ; (C) Ag^0 .

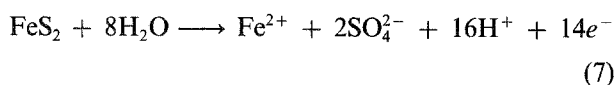
elemental silver would not be evident from the Ag(3d) spectrum, as the 3d binding energies are only 0.2 eV greater than those for silver sulphide.

The precipitated silver sulphide is expected to have a stoichiometry of Ag_{2.0}S. For the treated pyrite, the relative intensities of the Ag(3d)_{5/2} peak and the fitted S(2p) component at 161.3 eV, were the same as those for the precipitated silver sulphide and hence the stoichiometry of the altered layer was also Ag_{2.0}S. This is further evidence that no more than a small amount of elemental silver could have been present in the outermost few nanometres of the treated pyrite surface. Note that the results are not consistent with the formation of silver oxide since the former has Ag(MNN) energies 0.8 eV less than those for silver sulphide [18].

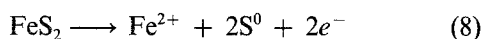
In contrast to the findings presented above, previous investigations of the pyrite/silver system under the same conditions [8, 12] were interpreted in terms of the development of a thick layer of elemental silver with only a minor quantity of silver sulphide being formed. However, the Ag(3d)_{5/2} binding energy and Ag(M₄NN) kinetic energy reported by these authors [8] were 368.0 and 356.6 eV, respectively. These values are close to the energies observed here for silver sulphide, so that the earlier XPS results would appear to be consistent with the formation of silver sulphide rather than elemental silver. Note that the values obtained in the present work for these parameters are in good agreement with those published previously [18–21].

Reaction between pyrite and silver ions to form silver sulphide and iron(II) ions does not account for all the sulphur atoms associated with the reacted mineral. Since no other surface sulphur species was detected under the above conditions, it must be concluded that some sulphur is oxidized to a soluble sulphur–oxygen anion. The latter is expected to be sulphate, since pyrite is known to yield both this species and sulphur on oxidation in acid solution [14].

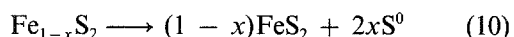
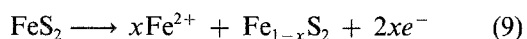
If the reaction of pyrite with silver ions is considered in terms of cathodic and anodic reactions, the latter will be represented by:



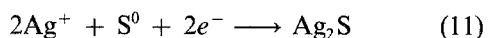
and



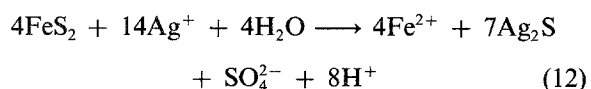
Reaction 8 occurs [22] via:



The cathodic reaction forming silver sulphide is:



For Ag₂S to be the only surface product, one pyritic sulphur atom in eight must oxidize to sulphate, *viz.*:



If fewer sulphur atoms than this ratio give rise to sulphate, elemental sulphur or a metal-deficient sulphide will be formed in addition to silver sulphide. On the other hand, if more than one in eight give sulphate, a cathodic process in addition to Reaction 11 must be invoked. The likely process is the formation of elemental silver:



The results presented above suggest that, under the conditions investigated, Reaction 12 is operative. The ratio of sulphate to sulphur formed in pyrite oxidation varies with changes in experimental conditions [14]. Thus, investigations were carried out at different temperatures and silver ion concentrations for various exposure times, with the aim of identifying whether conditions exist under which elemental sulphur or elemental silver is formed in association with silver sulphide.

When pyrite was immersed in a solution of the same composition as used above, *viz.* 0.25 mol dm⁻³ H₂SO₄, 10⁻² mol dm⁻³ Ag⁺, but exposed for 1 h at 298 K, a thinner altered layer developed and hence a larger proportion of unaltered pyrite remained at the surface. For example, Fe(2p) peaks from pyrite could be detected. The S(2p) spectrum after this treatment (Fig. 1E) could be fitted adequately by a doublet at 161.3 eV, accounting for 35% of the total S(2p) intensity, together with a doublet at the binding energy of unaltered pyrite. Thus, as after the higher treatment temperature, no elemental sulphur was detected. The Ag(MNN) spectrum was similar to that in Fig. 4A, indicating that most, if not all, of the silver was present as silver sulphide. The stoichiometry of this species, assuming that only sulphur with a 2p binding energy of 161.3 eV was bonded to silver, was Ag_{2.0}S and this also suggests negligible elemental silver is formed. Similar findings were obtained with the same temperature and exposure time when the Ag⁺ concentration was 10⁻³ mol dm⁻³.

Considerably less silver became incorporated into a pyrite surface immersed in 0.25 mol dm⁻³ H₂SO₄, 10⁻³ mol dm⁻³ Ag⁺ at 298 K for 5 min than for 1 h. Again, negligible elemental silver was detected. The S(2p) spectrum (Fig. 1F) includes a silver sulphide component that accounts for 20% of the intensity. The voltammetric investigations (Section 3.2) indicate that elemental sulphur or a metal-deficient sulphide was also produced under these conditions. There is no evidence from Fig. 1F for the presence of elemental sulphur, as there was no obvious component at 163.5 eV, and the S(2p) spectrum determined at 298 K was the same, within experimental error, as that determined at 150 K. However in this case, where the doublet from pyrite dominates the spectrum, it would not be possible to rule out the presence of a small component, with a binding energy between those of pyrite and elemental sulphur, due to lattice sulphur in metal-deficient sulphide environments [23]. It would be difficult to distinguish such a small component, when superimposed on the high binding energy base of the

doublet for the underlying pyrite, from an increase in the number of photoelectrons from pyrite suffering inelastic collisions due to the overlayer of silver sulphide. Again, assuming that only sulphur with a binding energy of 161.3 eV is bonded to silver, the stoichiometry of the silver sulphide formed on the mineral surface was $\text{Ag}_{1.7}\text{S}$. This stoichiometry could be explained by part of the low energy S(2p) intensity arising from the additional presence of a silver-iron sulphide or an iron sulphide such as pyrrhotite, which has a binding energy near 161.1 eV [24]. However, there is no evidence from the Fe(2p) spectrum for the presence of pyrrhotite; iron in this mineral is in the high-spin iron(II) form whereas it is low-spin iron(II) in pyrite. Voltammetry (Section 3.2) also gives no evidence of other metal sulphides being produced in addition to silver sulphide. A silver:sulphur atomic ratio of less than 2:1 could be explained by the structure of acanthite, the stable form of silver sulphide. Half the silver atoms in this structure are present in almost linear silver-sulphur chains, while the other silver atoms bind the chains together [25]. Thus, when only a few atomic layers of silver sulphide have been established, the average composition might be expected to be between Ag_2S and Ag_3S .

Prolonged immersion of pyrite at 298 K in 0.25 mol dm^{-3} H_2SO_4 containing 10^{-2} mol dm^{-3} Ag^+ resulted in a thinner altered layer than that formed on immersion for 2 h at 350 K, but the silver:sulphur ratio was now greater than 2:1. Figure 1G presents the S(2p) spectrum determined at 150 K from a surface treated for 15 h. The spectrum can be fitted by inclusion of a component at 161.3 eV in addition to that for pyritic sulfur, accounting for 50% of the total S(2p) intensity; there was no evidence for the presence of elemental sulphur. The silver:sulphur ratio of the silver-containing layer on this surface was estimated to be 2.1:1. This suggests that, under these conditions, some elemental silver may have been formed. However, there was no discernible difference in the Ag(MNN) spectrum from that recorded for precipitated silver sulphide. It is conceivable that a contribution from up to 10% of elemental silver might not be apparent in the Auger spectrum because of the broad line-widths.

Interaction of pyrite with silver ions to form silver sulphide is not dependent on the solution having a low pH. A surface immersed in unacidified 10^{-3} mol dm^{-3} Ag^+ for 10 min at 298 K became as enriched in silver as one immersed for 1 h in 0.25 mol dm^{-3} H_2SO_4 containing 10^{-3} mol dm^{-3} Ag^+ . Elemental sulphur was not detected and the Ag(MNN) Auger spectrum showed the silver to be present as silver sulphide.

When a surface pretreated in silver solution was leached for 30 min at 350 K in 0.25 mol dm^{-3} H_2SO_4 containing 1 mol dm^{-3} $\text{Fe}_2(\text{SO}_4)_3$ (but no silver ions), the S(2p) spectrum determined at 150 K (Fig. 1H) confirmed the expected production of elemental sulphur [8]. A small amount of sulphate was also retained at the surface. Most of the elemental sulfur layer, which was insufficiently thick or uniform to mask the underlying pyrite, was lost to the spectrometer vacuum soon after

the specimen was allowed to warm to 298 K. Only a very small concentration of silver remained at the leached pyrite surface; Ag(3d) peaks could just be detected whereas Ag(MNN) peaks could not. This is consistent with the absence of a detectable component at 161.3 eV in the S(2p) spectrum. The removal of most of the silver from the pyrite surface under iron(III) leaching conditions is in agreement with previous observations [8].

3.2. Voltammetry

Figure 5, curve A, presents a voltammogram for a pyrite electrode in 0.25 mol dm^{-3} sulphuric acid solution. The sweep was commenced at the open circuit potential and taken initially in the positive-going direction. The anodic current observed in the high potential region is due to oxidation of pyrite to sulphur or sulfate with iron entering the solution as iron(II) or iron(III) species [14]. The surface sulphur product under these conditions is probably a metal-deficient pyrite rather than a separate elemental sulphur phase [23]. On the subsequent negative-going scan, a cathodic peak appears at about 0 V; this arises from the reduction of surface sulfur formed on the pyrite by oxidation during exposure to air and, to a minor extent, during the excursion to high potentials on the sweep. As the lower potential limit is approached, a rising cathodic current is observed due to the reduction of pyrite itself. When the scan is again reversed, an anodic peak is observed at about 0.3 V due to oxidation of the H_2S formed by reduction of sulfur on the preceding scan. This peak was eliminated when the electrode was rotated to disperse the H_2S from the electrode surface.

The voltammogram shown in Fig. 5, curve B was obtained after the solution was made 10^{-3} mol dm^{-3} in silver ions and the electrode left at open circuit for 2 h. It can be seen that the open circuit potential was shifted to more positive potentials by the addition of silver ions and that the anodic current on the first positive-going scan was less than that observed for pyrite in the absence of Ag^+ . The subsequent negative-going scan displays a peak at about 0.5 V due to the

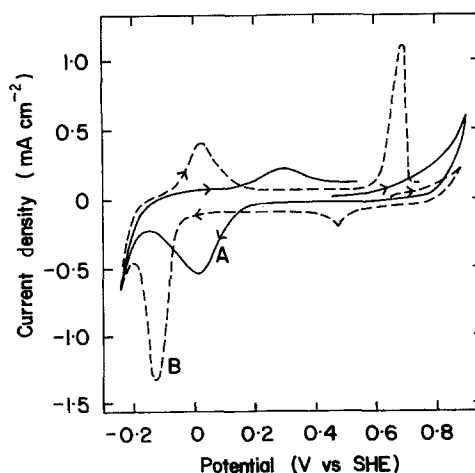


Fig. 5. Voltammograms for pyrite electrode in: (A) 0.25 mol dm^{-3} H_2SO_4 ; (B) 0.25 mol dm^{-3} H_2SO_4 , 10^{-3} mol dm^{-3} Ag^+ after 2 h at open circuit. Sweep rate 20 mV s^{-1} .

deposition of elemental silver and the current then takes up the mass transport-limited value for this reaction. A large cathodic peak appears at about -0.1 V and this can be assigned [13] to reduction by Reaction 6 of silver sulphide formed by interaction of pyrite with Ag^+ . On the second positive-going scan, an anodic peak is observed due to the reverse of Reaction 6. This peak disappeared when the electrode was rotated, substantiating the assignment. Finally, it can be seen that an anodic peak appears at about 0.7 V due to dissolution of silver electrodeposited in the low potential region.

No peak due to the dissolution of silver is apparent on the first positive-going scan in Fig. 5, curve B and hence no elemental silver was formed by reaction of pyrite with Ag^+ under the conditions of that experiment. Thus, the electrochemical studies confirm the conclusion made from the XPS investigations (Section 3.1) that Ag_2S is the only surface reaction product under such conditions. However, this result differs from that reported previously [12] in which elemental silver was identified as the principal product. This discrepancy could be due to the fact that, in the earlier work, the potential was held at a value equivalent to the measured rest potential, which was close to the reversible potential of the Ag/Ag^+ system. If the potential at which the electrode was held was only a few millivolts below the actual rest potential and was in the silver deposition region, then silver will be deposited electrochemically rather than by reaction of silver ions with the pyrite.

As pointed out in Section 3.1, the formation of Ag_2S from FeS_2 by exchange of Fe^{2+} for Ag^+ does not account for all the sulphur atoms in the pyrite reacted. There is no evidence in Fig. 5 for the presence of elemental sulphur or excess sulphur in the pyrite lattice in the form of a metal-deficient sulphide. However, such species could react with silver ions during the potential scan by the reverse of Reaction 5 and hence only Ag_2S would be detected. Thus, experiments were carried out in which the electrode was immersed in the silver-containing solution for a specified time and then transferred to another cell where voltammetry was carried out in 0.25 mol dm^{-3} sulphuric acid alone. Figure 6 shows scans commenced in the negative-

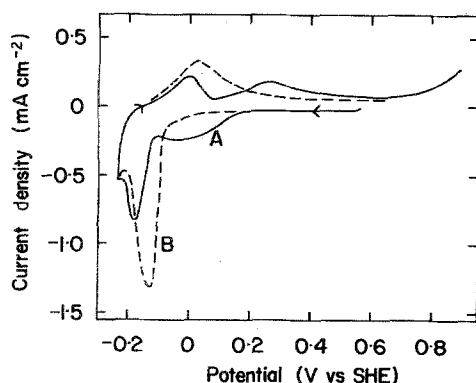


Fig. 6. Voltammograms for pyrite electrode in 0.25 mol dm^{-3} H_2SO_4 after immersion in 0.25 mol dm^{-3} H_2SO_4 , $10^{-3} \text{ mol dm}^{-3}$ Ag^+ at 298 K for: (A) 30 s; (B) 30 min. Sweep rate 20 mV s^{-1} .

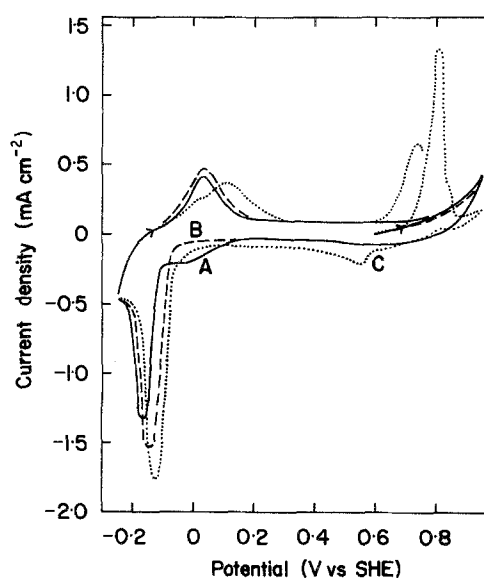


Fig. 7. Voltammograms for pyrite electrode in 0.25 mol dm^{-3} H_2SO_4 after immersion in 0.25 mol dm^{-3} H_2SO_4 , $10^{-2} \text{ mol dm}^{-3}$ Ag^+ at 298 K for: (A) 5 min; (B) 30 min; (C) 17 h. Sweep rate 20 mV s^{-1} .

going direction so that no oxidation of the electrode surface could occur following the treatment with silver ions. It can be seen that, after 30 s immersion, there is a peak corresponding to the reduction of sulphur in addition to that for Ag_2S reduction. The XPS studies presented in Section 3.1 suggest that this sulphur is present as metal-deficient (sulphur-rich) environments in the sulphide lattice; the $\text{S}(2p)$ spectrum of a pyrite surface immersed in a silver solution for 5 min was not inconsistent with such species but clearly showed elemental sulphur to be absent. Figure 6 shows that the metal-deficient sulphide is no longer apparent after 30 min treatment.

The results shown in Fig. 7, in which the electrode was immersed in 0.25 mol dm^{-3} H_2SO_4 , $10^{-2} \text{ mol dm}^{-3}$ Ag^+ and scans run in 0.25 mol dm^{-3} H_2SO_4 , show only a small sulphur peak for 5 min immersion and a negligible quantity for 30 min. All the voltammetric peaks can be assigned on the basis of the development of silver sulphide and there is no evidence for the presence of other species. In particular, there is no indication of elemental silver on these scans. Again, the electrochemical findings are in agreement with the XPS results. However, the voltammogram in Fig. 7 recorded after immersion for 17 h displays an anodic peak on the initial, positive-going scan at about 0.8 V and this corresponds to silver dissolution. The assignment of this peak to silver dissolution is substantiated by the appearance of a cathodic peak at about 0.55 V on the following negative-going scan due to re-plating of the dissolved silver. The formation of elemental silver was also observed following immersion of pyrite for 1 h in 0.25 mol dm^{-3} H_2SO_4 , $10^{-2} \text{ mol dm}^{-3}$ Ag^+ at 350 K (Fig. 8).

The latter finding is in agreement with the report [8] that silver metal could be detected by XRD analysis after similar treatment. However, silver metal is not associated with the appearance of elemental sulphur as expected by Reaction 3. Elemental silver

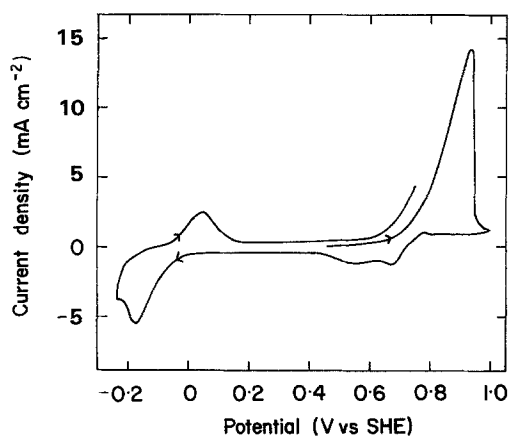


Fig. 8. Voltammogram for pyrite electrode in $0.25 \text{ mol dm}^{-3} \text{ H}_2\text{SO}_4$ after immersion in $0.25 \text{ mol dm}^{-3} \text{ H}_2\text{SO}_4$, $10^{-2} \text{ mol dm}^{-3} \text{ Ag}^+$ for 1 h at 350 K. Sweep rate 20 mV s^{-1} .

is only produced when elemental sulphur is absent; this is as expected from the proposed mechanism (Reactions 7–13).

Voltammetric investigations were also carried out on pyrite surfaces after immersion in $0.25 \text{ mol dm}^{-3} \text{ H}_2\text{SO}_4$, $10^{-2} \text{ mol dm}^{-3} \text{ Ag}^+$, $1 \text{ mol dm}^{-3} \text{ Fe}_2(\text{SO}_4)_3$ at 350 K. Peaks for sulphur and silver sulphide were observed under all conditions studied, but none corresponding to elemental silver. For solid electrodes, these peaks were masked to some extent by reactions of soluble iron species which presumably had ingressed into cracks, formed between the mineral and surrounding epoxy resin during temperature changes, when the electrode was in the leach solution. To avoid this problem, studies were also carried out on pyrite particles using a carbon paste electrode. Figure 9 shows a voltammogram recorded after immersion for 5 min; cathodic peaks at about 0 V and -0.15 V , associated with sulphur and silver sulphide reduction, respectively, are clearly displayed. There is no evidence on the initial positive-going scan for the presence of elemental silver. Indeed, the rest potential of the electrode after treatment in the iron solution was about 0.67 V , which is significantly above the potential at which silver will dissolve. Note that an anodic peak due to silver dissolution appears on the second positive-going scan. This arises because the

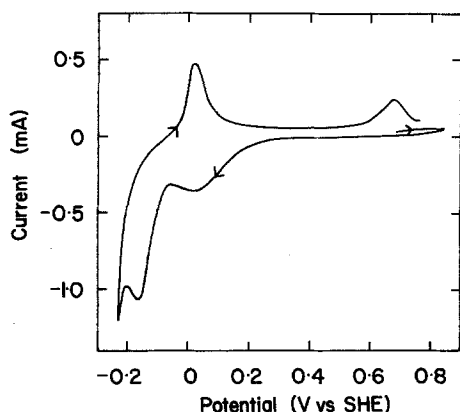


Fig. 9. Voltammogram for pyrite particles incorporated in carbon paste electrode after treatment of the mineral in $0.25 \text{ mol dm}^{-3} \text{ H}_2\text{SO}_4$, $10^{-2} \text{ mol dm}^{-3} \text{ Ag}^+$, $1 \text{ mol dm}^{-3} \text{ Fe}_2(\text{SO}_4)_3$ for 5 min at 350 K. Sweep rate 10 mV s^{-1} .

silver sulphide is reduced to Ag^0 and H_2S during the prior excursion to low potentials. The major portion of the silver re-forms Ag_2S giving rise to the anodic peak at about 0 V , but there is excess Ag^0 because some of the H_2S diffuses away from the electrode surface.

3.3. Scanning electron microscopy

As discussed above, elemental silver was not detected by XPS on surfaces treated in the same manner as those corresponding to Fig. 7C and Fig. 8, which clearly show this species to be present. In the latter case, the difference could be due to the thick layer of silver sulphide formed, since only the outer few nanometres are examined by XPS. However, in the former situation, peaks from the underlying pyrite were also observed and hence all species in the overlayer should be detectable. In order to reconcile these differences, a pyrite surface after immersion in $0.25 \text{ mol dm}^{-3} \text{ H}_2\text{SO}_4$, $10^{-2} \text{ mol dm}^{-3} \text{ Ag}^+$ for 7 days was examined under the SEM. Elemental analysis showed that some silver was present over all the surface and this layer was presumably Ag_2S . There were also features on the surface as shown in Fig. 10 that appeared bright in the back-scattered electron image. These features were of the order of a micrometre in size and hence analysis in the SEM without including some signal from the surrounding material was not possible. However, elemental analysis of the largest crystals showed that the silver must be present in the metallic form. Presumably, nucleation and growth of silver crystals occurs on a restricted number of sites. This results in crystals of elemental silver $\leq 3 \mu\text{m}$ in size forming on the pyrite surface and covering only a few per cent of the exposed area. Such crystals were readily detected voltammetrically, since this technique is responsive to the total number of electroactive atoms or molecules on the electrode surface. However, these crystals were not discernible by XPS, which examines the first few atomic layers over a relatively large surface area, since the elemental silver had to be differentiated from the evenly distributed silver sulphide.

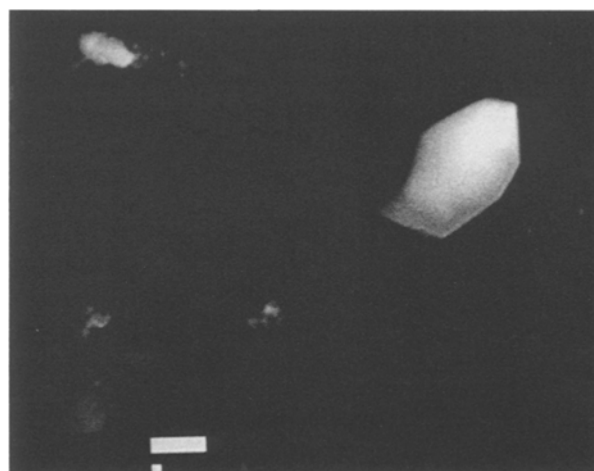


Fig. 10. Electron micrograph showing silver crystals formed on a pyrite surface after immersion in $0.25 \text{ mol dm}^{-3} \text{ H}_2\text{SO}_4$, $10^{-2} \text{ mol dm}^{-3} \text{ Ag}^+$ for 7 days. Bar represents $1 \mu\text{m}$.

4. Conclusions

It has been demonstrated that silver sulphide, elemental silver and elemental sulphur can be individually identified on a pyrite surface from the characteristics of electron spectra and of voltammograms. Studies of the interaction of pyrite with solutions containing silver ions utilizing both these techniques have shown that the initial product is silver sulphide together with a metal-deficient (sulphur excess) pyrite surface. Further reaction results in a thicker silver sulphide layer together with loss of the excess sulphur from the pyrite.

Voltammograms recorded after immersion of pyrite surfaces in silver solutions at 298 K for extended periods, or after treatment of the mineral in such solutions at 350 K, revealed that elemental silver was formed in addition to silver sulphide. In contrast, electron spectra from such surfaces failed to detect silver in the elemental form. SEM examination of surfaces after extended exposure to silver ions at 298 K provided an explanation of this discrepancy. Nucleation and growth of silver crystals occurred on a restricted number of sites on the mineral surface and hence elemental silver could be present in significant quantities, but on only a few per cent of the area, whereas silver sulphide covered the whole of the specimen.

It is concluded that the sulphur atoms of the reacted pyrite that are not associated with the silver sulphide product are transferred to the solution phase as sulphate ions. This mechanism explains the formation under different conditions of silver sulphide plus sulphur, silver sulphide alone, or elemental silver plus silver sulphide in terms of the fraction of pyritic sulphur atoms oxidized to sulphate. It also accounts for the fact that elemental silver and elemental sulphur were never detected on the same surface.

When a pyrite surface that had been reacted with silver ions was immersed in an acidic iron(III) solution at 350 K, the silver was dissolved and elemental sulphur developed on the mineral surface. Treatment of pyrite at 350 K with such a solution containing silver ions resulted in silver sulphide and sulphur being formed.

Acknowledgement

The authors thank Mr P. Rummel of the CSIRO Division of Mineral Products for the SEM investigations.

References

- [1] E. Peters, in 'Electrochemistry in Mineral and Metal Processing' (edited by P. E. Richardson, S. Srinivasan and R. Woods), The Electrochem. Soc., Pennington, NJ (1984) pp. 343-361.
- [2] M. Ammou-Chokroum, A. M. Steinmetz and A. Malve, *Bull. Mineral.* **101** (1978) 26.
- [3] A. J. Parker, R. L. Paul and G. P. Power, *J. Electroanal. Chem.* **118** (1981) 305.
- [4] H. G. Linge, *Hydrometallurgy* **2** (1976) 51.
- [5] A. N. Buckley, H. J. Wouterlood and R. Woods, *Hydrometallurgy* **22** (1989) in press.
- [6] J. D. Miller and H. Q. Portillo, in 'Mineral Processing' (edited by J. Laskowski), Elsevier, Amsterdam (1981) pp. 851-901.
- [7] J. S. Niederkorn, *J. Met.* **37** (1985) 53.
- [8] J. B. Hiskey, P. P. Phule and M. D. Pritzker, *Metall. Trans. B* **18B** (1987) 641.
- [9] W. M. Moore and P. J. Codella, *J. Phys. Chem.* **92** (1988) 4421.
- [10] A. W. Czanderna, *J. Phys. Chem.* **68** (1964) 2765.
- [11] J. Horvath and M. Novak, *Corros. Sci.* **4** (1964) 159.
- [12] J. B. Hiskey and M. D. Pritzker, *J. Appl. Electrochem.* **18** (1988) 484.
- [13] D. W. Price, G. W. Warren and B. Drouven, *J. Appl. Electrochem.* **16** (1986) 719.
- [14] I. C. Hamilton and R. Woods, *J. Electroanal. Chem.* **118** (1981) 327.
- [15] A. N. Buckley, R. Woods and H. J. Wouterlood, *Aust. J. Chem.* **41** (1988) 1003.
- [16] A. N. Buckley, I. C. Hamilton and R. Woods, *J. Appl. Electrochem.* **14** (1984) 63.
- [17] R. G. Bates, 'Determination of pH', Wiley, New York (1964) pp. 458-483.
- [18] M. Romand, M. Roubin and J. P. Deloume, *J. Electron Spectrosc.* **13** (1978) 229.
- [19] D. Lichtman, J. H. Craig, V. Sailer and M. Drinkwine, *Appl. Surf. Sci.* **7** (1981) 325.
- [20] G. Remond, P. H. Holloway, C. T. Horland and R. R. Olson, *Scanning Electron Microsc.* (1982) 995.
- [21] T. M. H. Saber and A. A. El Warraky, *Br. Corros. J.* **23** (1988) 131.
- [22] A. N. Buckley and R. Woods, *Appl. Surf. Sci.* **27** (1987) 437.
- [23] A. N. Buckley, I. C. Hamilton and R. Woods, in 'Electrochemistry in Mineral and Metal Processing II' (edited by P. E. Richardson and R. Woods), The Electrochem. Soc., Pennington, NJ (1988) pp. 234-246.
- [24] A. N. Buckley and R. Woods, *Appl. Surf. Sci.* **22/23** (1985) 280.
- [25] D. J. Vaughan and J. R. Craig, 'Mineral Chemistry of Metal Sulfides', Cambridge University Press (1978) p. 59.